

Uncovering microscopic details of shearing mechanisms in the L1₂ structure by unambiguous stacking fault analysis

Nicolas Karpstein¹, Malte Lenz¹, Andreas Bezold², Rico Zehl³, Mingjian Wu¹, Alfred Ludwig³, Guillaume Laplanche³, Steffen Neumeier², Erdmann Spiecker¹

¹Friedrich-Alexander-Universität Erlangen-Nürnberg, Department of Materials Science & Engineering, Institute of Micro- and Nanostructure Research, and Center for Nanoanalysis and Electron Microscopy (CENEM), Erlangen, Germany, ²Friedrich-Alexander-Universität Erlangen-Nürnberg, Department of Materials Science & Engineering, Institute I: General Materials Properties, Erlangen, Germany, ³Ruhr-Universität Bochum, Institut für Werkstoffe, Bochum, Germany

Background incl. aims

γ/γ' -strengthened Ni- and Co-base superalloys for applications at high temperatures rely on the precipitation-strengthening effect of the L1₂-ordered γ' phase embedded into the face-centered cubic γ matrix phase. Therefore, the microscopic mechanisms by which the γ' phase can be sheared crucially influence the mechanical properties of the alloy, and their understanding is of key importance. In this context, an established method to discriminate between intrinsic and extrinsic stacking faults (SFs) is their edge-on imaging in high-resolution scanning transmission electron microscopy (HRSTEM) in $\langle 110 \rangle$ projection. The superlattice ordering within the L1₂ phase gives rise to a larger variety of fault structures – namely, complex and superlattice variants of both intrinsic and extrinsic stacking faults. Notably, whether a given SF is complex or not may not be reliably revealed by studying one $\langle 110 \rangle$ projection alone [1, 2]. We present an experimentally feasible approach that enables this differentiation in a reliable and unambiguous way. This approach entails examining the fault structure not only in $\langle 110 \rangle$ projection, but also in a neighboring $\langle 211 \rangle$ projection, which is achieved by tilting the specimen by 30° in the TEM. Two applications of this analysis technique are discussed in this contribution: the first is the experimental validation of microscopic details of a well-known formation mechanism for superlattice extrinsic stacking faults, and the second concerns the shear-based γ' -to- χ phase transformation often observed in superalloys based on the Co-Al-W system, in which χ is an equilibrium phase [3].

Methods

Fault structures in the single crystalline Co-base superalloys ERBOCo-4 (composition in at.-%: Co43.2-Ni32.0-Al8.0-Cr6.0-Ti2.8-Si0.4-Hf0.1-Ta1.8-W5.7) and ERBOCo-VF60 (composition in at.-%: Co79.8-Al8.9-Ta2.3-W9.0) are analyzed. HRSTEM imaging was performed at a double Cs-corrected FEI Titan³ Themis at 300 kV as well as a probe-corrected Thermo Fisher Scientific Spectra 200 C-FEG at 200 kV. On the latter, spatially resolved energy-dispersive X-ray spectroscopy (EDXS) was conducted using the Super-X G2 detector.

Results

The first example concerns a high-temperature deformation mechanism of the γ' phase which involves the formation of SFs. Details of this study can be found in Ref. [2] and are briefly summarized in the following. Under [001] compression, a common deformation mode resulting in the formation of superlattice extrinsic SFs (SESFs) is the well-known Kolbe mechanism [4]. Here, two identical $a/6\langle 112 \rangle$ Shockley partial dislocations shear into γ' on neighboring planes, leaving behind two neighboring complex intrinsic SFs (CISFs) which together constitute a complex extrinsic SF (CESF). Complex variants of SFs typically possess high SF energies due to nearest-neighbor violations in the superlattice ordering; therefore, the central fault plane of the CESF undergoes a diffusion-mediated reordering step which effectively translates that plane by $a/2\langle 110 \rangle$ and transforms the fault into a lower-energy SESF. While numerous observations of this mechanism have been made in Ni- and Co-base

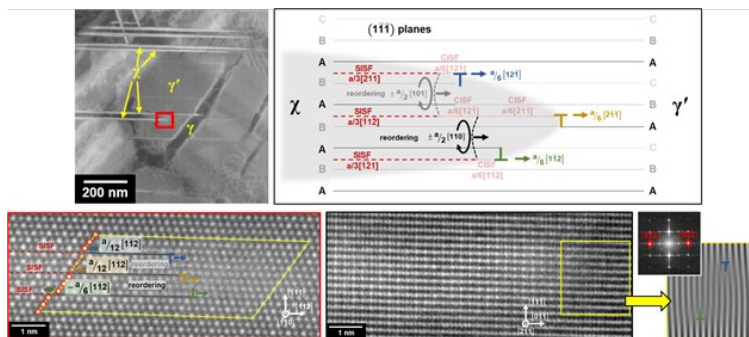
superalloys since its model description in 2001, two key aspects have previously eluded experimental verification: firstly, a direct observation of the complex nature of the intrinsic segment between the two leading partials, and secondly, the occurrence of reordering. By imaging the fault structure and leading partials in a compressively deformed sample of Co-base superalloy ERBOCo-4 not only in $\langle 110 \rangle$ projection (which may be ambiguous regarding the complex or superlattice character of a fault), but also in $\langle 211 \rangle$ projection, we were able to reveal the intrinsic and extrinsic segments as CISF and SESF, respectively, directly confirming both aforementioned aspects [2].

In the second example, microscopic details of the $\gamma'(L1_2)$ -to- $\chi(D0_{19})$ phase transformation were elucidated in the Co-base superalloy ERBOCo-VF60 (see figure). The accelerated formation of the χ phase during annealing (850 °C, 20 h) was prompted by the diffusion of Cr into the superalloy, destabilizing the γ/γ' microstructure. Coherent, plate-shaped χ precipitates have formed on $\{111\}$ planes. Based on the fcc-to-hcp transformation, the transformation of the $L1_2$ structure (ABC stacking) to the $D0_{19}$ structure (AB stacking) is shear-based and can be achieved by the introduction of an SISF after every other plane of the $L1_2$ structure. By studying the leading partials driving the transformation at the tip of a precipitate in HRSTEM, details of the transformation process were uncovered [5]. In $[110]$ projection (bordered in red), the formation of SFs is evident, causing a change in stacking. Furthermore, a change in the alternating bright/dark contrast of atomic columns on the planes marked by dashed red circles implies the involvement of a diffusion-mediated reordering process. By additionally imaging the fault structure in $[211]$ projection (bordered in black), the Burgers vectors of the leading partials were determined unambiguously (from superlattice shifts made visible by Fourier filtering in this projection) as noted in the schematic drawing. Notably, the transformation does not progress directly through shearing by $a/3\langle 112 \rangle$ partials necessary to form SISFs, but rather by $a/6\langle 112 \rangle$ partials which leave behind CISFs. The smaller Burgers vectors facilitate shearing and reduce elastic strains at the transformation front. At the same time, the high-energy CISFs are transformed into lower-energy SISFs by reordering processes. As illustrated in the schematic drawing, this fault configuration can serve to transform the ABC stacking of γ into the AB stacking of χ . The sum of all translation vectors in this configuration, and therefore the net strain introduced into the microstructure, is zero. Fault configurations following this pattern of three $a/6\langle 112 \rangle$ partials creating CISFs followed by reordering to SISFs were observed repeatedly at the transformation fronts, indicating that this may be the preferred transformation mechanism. Besides the change in crystal structure, the formation of the χ phase also involves a significant enrichment of W and Ta supplied by diffusion from the surrounding microstructure. An in-depth characterization and discussion of elemental distributions associated with this phase transformation was conducted based on EDXS measurements down to the atomic scale.

Conclusion

We have presented two experimental applications of a novel HRSTEM-based method to reliably and unambiguously identify the complex or superlattice nature of both intrinsic and extrinsic SFs in the $L1_2$ structure. In both cases, microscopic details of shearing mechanisms in the γ' phase of high-temperature superalloys were elucidated. In the future, this method may help uncover the details behind other $L1_2$ shearing processes.

Graphic:



Keywords:

Scanning-transmission-electron-microscopy, superalloys, stacking-faults, deformation-mechanisms, phase-transformations

Reference:

- [1] P.M. Sarosi, G.B. Viswanathan, M.J. Mills, Scripta Mater 55(8) (2006) 727-730.
- [2] N. Karpstein, M. Lenz, A. Bezold, M. Wu, S. Neumeier, E. Spiecker, Acta Mater 260 (2023) 119284.
- [3] Y.Z. Li, F. Pyczak, M. Oehring, L. Wang, J. Paul, U. Lorenz, Z. Yao, J Alloy Compd 729 (2017) 266-276.
- [4] M. Kolbe, Mat Sci Eng a-Struct 319 (2001) 383-387.
- [5] N. Karpstein, A. Saksena, R. Zehl, A. Bezold, O.M. Horst, D. Bürger, A. Kostka, C. Zenk, S. Neumeier, B. Gault, A. Ludwig, S.G. Fries, G. Laplanche, E. Spiecker, Manuscript in preparation.